APPLIED SCIENCES AND ENGINEERING

A coating from nature

Johannes G. H. Hermens[1], Thomas Freese[1], Keimpe J. van den Berg[2], Rogier van Gemert[2], Ben L. Feringa[1]*

For almost a century, petrochemical-based monomers like acrylates have been widely used as the basis for coatings, resins, and paints. The development of sustainable alternatives, integrating the principles of green chemistry in starting material, synthesis process, and product function, offers tremendous challenges for science and society. Here, we report on alkoxybutenolides as a bio-based alternative for acrylates and the formation of high-performance coatings. Starting from biomass-derived furfural and an environmentally benign photochemical conversion using visible light and oxygen in a flow reactor provides the alkoxybutenolide monomers. This is followed by radical (co) polymerization, which results in coatings with tunable properties for applications on distinct surfaces like glass or plastic. The performance is comparable to current petrochemical-derived industrial coatings.

INTRODUCTION

Coatings are omnipresent in daily life, indispensable in construction and applied to enhance properties and durability of numerous products, ranging from cans to cars (*1*). The polymers and resins in coatings are manufactured using petrochemical feedstock (*2*). However, the environmental awareness and the need to design the green chemistry of the future based on sustainable materials demand for renewable resources and waste-free, low-energy chemical conversions without compromising the function and performance of the final products (*3*–*5*). In the multistep processes that are typically used nowadays, middle- to long-chain fossil-based hydrocarbons are converted into olefins via cracking, further oxidized and derivatized into acrylates, which are subsequently polymerized to yield a wide range of plastics, resins, and coatings (Fig. 1A) (*6*). Global production of acrylate esters exceeds 3.5 million metric tons a year (*7*), and it is evident that sustainable alternatives, maintaining the favorable properties of acrylate-based materials, can be highly transformative in tomorrow's chemistry and materials. Despite progress toward the use of renewable feedstock for fuels (*8*), polymers (*9*–*11*), and specialty chemicals (*12*, *13*), as well as recent advances in photoredox (*14*) and electrochemical conversions (*15*, *16*) aiming at the design of benign and low waste transformations (*17*, *18*), direct biomass-derived alternatives for acrylate-based coatings remain largely unexplored (*18*–*23*). Although bio-based polyesters are now well established (*9*), limited reports on (co)polymerization of acrylate analogs did not reveal materials function (*24*) or indicated large differences in reactivity compared with common acrylates (*25*). Here, we demonstrate the formation of high-performance coatings using lignocellulose-derived alkoxybutenolides as an alternative for acrylates while using a photooxidation process with visible light and oxygen in a scalable flow system to access the monomers.

In our design, shown in Fig. 1A, implementing the Principles of Green Chemistry (*26*), we take an integrated approach using a renewable resource, green transformations, intrinsic functionality for polymerization, and tunable materials properties of the coatings. The starting point is biomass, e.g., lignocellulose, which is readily converted into valuable platform chemicals like furfural using acid-mediated dehydration (Fig. 1A) (*27*). The next step is a photooxidation based on singlet oxygen ($^1O_2$), which is generated using visible light and a catalytic triplet sensitizer. This particularly clean process involves triplet-triplet annihilation of the excited photosensitizer and molecular oxygen. The furan moiety of furfural undergoes a [4 + 2] cycloaddition with $^1O_2$ and transforms quantitatively into hydroxybutenolide, which can be readily converted into various alkoxybutenolides by heating with the appropriate alcohol (Fig. 1B). The alkoxybutenolide structure has an embedded acrylate functionality (depicted in pink in Fig. 1A). Extensive earlier studies in our group, using these compounds as chiral maleic anhydride–type building blocks in natural product synthesis (*28*, *29*), revealed the reactivity of the α,β-unsaturated ester unit most likely to be intermediate between that of crotonate and acrylate monomers. The cisoid configuration of the alkene moiety in the butenolide and the electronic effect of the acetal group contribute to this distinct reactivity. We envisioned that the butenolides can be directly used as monomers in (co)polymerizations and resin formation replacing acrylates. Furthermore, the use of various (linear and branched) alcohols in the acetal formation step readily provides a range of alkoxybutenolide monomers, allowing the formation of coatings with tunable materials properties (Fig. 1B). Here, we deliver methodology to access the key butenolide monomers in an (industrial) scalable process and demonstrate their ability to form high-quality coatings, substantially reducing our environmental footprint.

RESULTS AND DISCUSSION

Monomer formation

In preliminary studies on the photooxidation of furfural using 6 mole percent (mol %) of methylene blue as triplet sensitizer and visible light (λ_{irr} = 635 nm) in an immersion well reactor, we could selectively produce hydroxybutenolide **B1** up to a 500-mmol scale without requiring further purification (Fig. 2A) (see Materials and Methods and the Supplementary Materials pages S4, S248, and S249 for experimental details and product characterization). Facing the challenge to upscale this singlet oxygen photochemical reaction (*30*) to provide sufficient quantities of butenolide monomers for coating formation, we focused on rotating thin-film techniques (Fig. 2B) and flow photoreactors (Fig. 2C). To overcome the problem of limited light penetration in solution, as transmittance of light decreases

[1]Advanced Research Centre CBBC, Stratingh Institute for Chemistry and Zernike Institute for Advanced Materials, Faculty of Science and Engineering, University of Groningen, Nijenborgh 4, Groningen, 9747 AG, Netherlands. [2]Department Resin Technology, Akzo Nobel Car Refinishes BV, Sassenheim, 2171 AJ, Netherlands.
*Corresponding author. Email: b.l.feringa@rug.nl

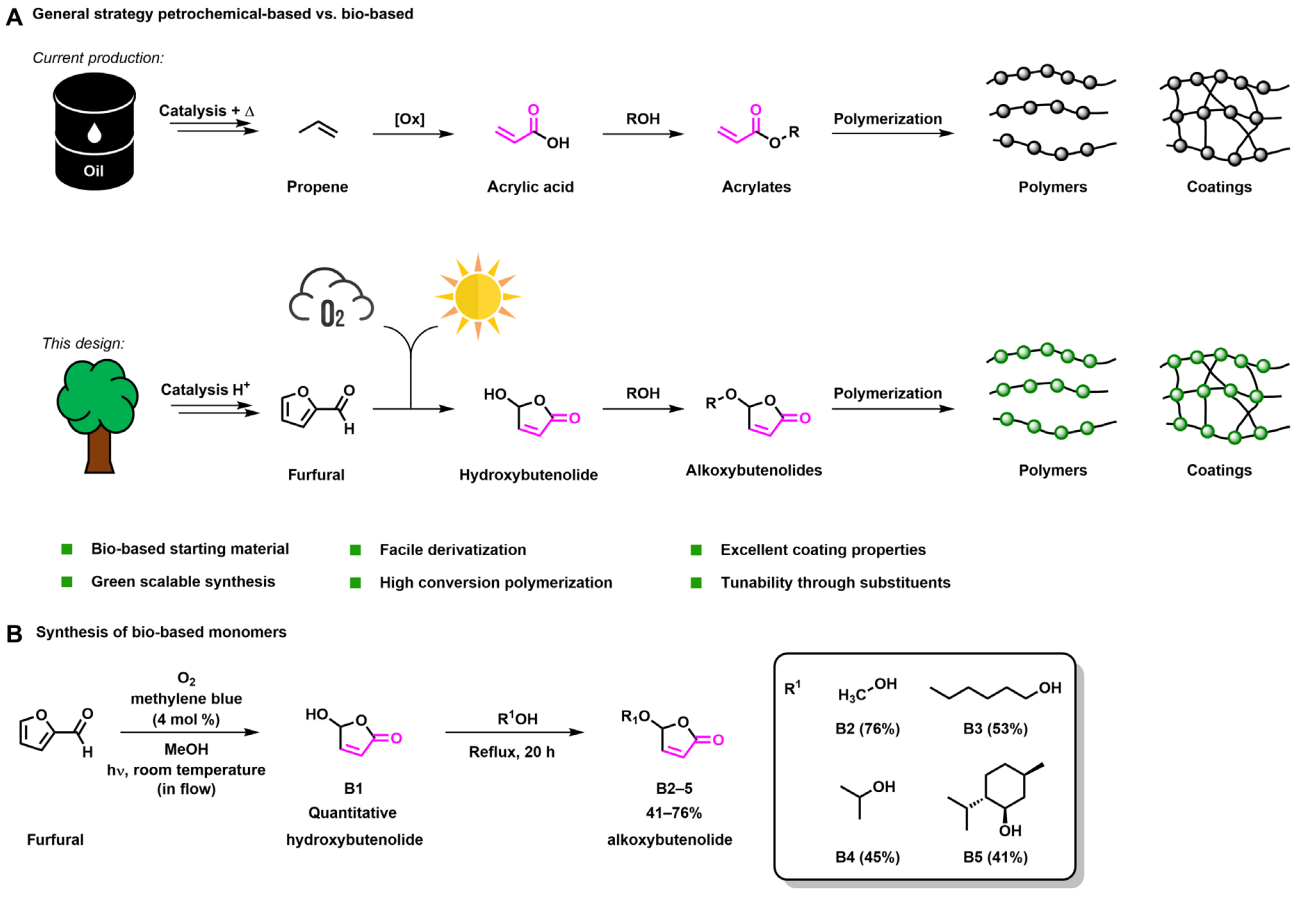

Fig. 1. Design of bio-based alternatives for acrylates and coatings. (**A**) General strategy for bio-based alternatives instead of common petrochemical-based acrylate monomers to yield coatings. (**B**) Photooxidation of the biomass-derived furfural followed by derivatization toward alkoxybutenolide monomers comprising an acrylate type structure (acrylate unit is shown in pink).

exponentially with distance (*30*), thin films allow homogeneous photon flux and enhanced efficacy. In addition, flow chemistry is particularly attractive for photooxygenation dealing with multiphase reaction mixtures (gas-liquid), which are often limited by mass transfer (*31*).

A rotary evaporator photoreactor, modeled after Poliakoff and George (*32*), allows the continuous creation of a flow and thin film through fast rotation of the flask for optimal light penetration and O_2 transfer into the solution (Fig. 2B). Optimization of this system with respect to reactor flask size, volume, concentrations, and light source showed that a 1-liter flask with a small volume of 10 ml (1 M solution, 0.45 mol % methylene blue) resulted in full conversion within 20 min, which corresponds to a production of 30 mmol/hour of **B1** (for optimization, see table S1).

Although this single rotary photoreactor enabled us to produce over 1 kg of hydroxybutenolide **B1**, operating this initial setup is a noncontinuous process, because it was not computer controlled like the original setup of George and co-workers (*32*). In an alternative approach, a photochemical flow system was explored on the basis of the original reactor design of Booker-Milburn (*33*) and taking inspiration from the studies on flow photooxidation reactions by Seeberger (*34*). This system was constructed by simply wrapping fluorinated ethylene propylene (FEP) tubing around a glass tube surrounding a standard 18-W TL bulb to retain room temperature (Fig. 2C). The substrate solution containing furfural and 4 mol % of methylene blue, dissolved in preoxygenated methanol, was added via a dosing pump, and a flow of oxygen was applied. Upon combination of the flows in the T-piece, an intermittent sequence of small gas and liquid bubbles is created, which results in efficient mixing. Optimal light penetration is achieved because of the thin tubing (1.59 mm internal diameter), creating small volumes of solution. The reaction was optimized for flow rate, residence time, and photocatalyst loading. Under the optimized conditions, hydroxybutenolide **B1** was selectively produced at 1.5 mmol/hour. A convenient strategy for increasing the scale of these continuous flow setups is by multiplying the setup in parallel (*35*, *36*). As a result of this continuous flow setup being simple and small, it can be duplicated many times, readily enhancing the production. Figure 2C illustrates five photoflow reactors in parallel in a single fume hood setup allowing continuous formation of hydroxybutenolide **B1** at a rate of 7.5 mmol/hour.

With a continuous flow photooxidation process to form hydroxybutenolide **B1** in operation, the next step involved the introduction of distinct alkoxy substituents to provide various butenolide monomers. We envisioned that this would allow tuning of the materials properties upon polymerization (Fig. 1B). Taking advantage of the cyclic hemiacetal moiety (a masked aldehyde) in **B1**, simply heating this compound in the presence of the appropriate alcohol provided alkoxybutenolides **B2** to **B5**. These condensation reactions can readily be performed on a 100-g scale, and representative

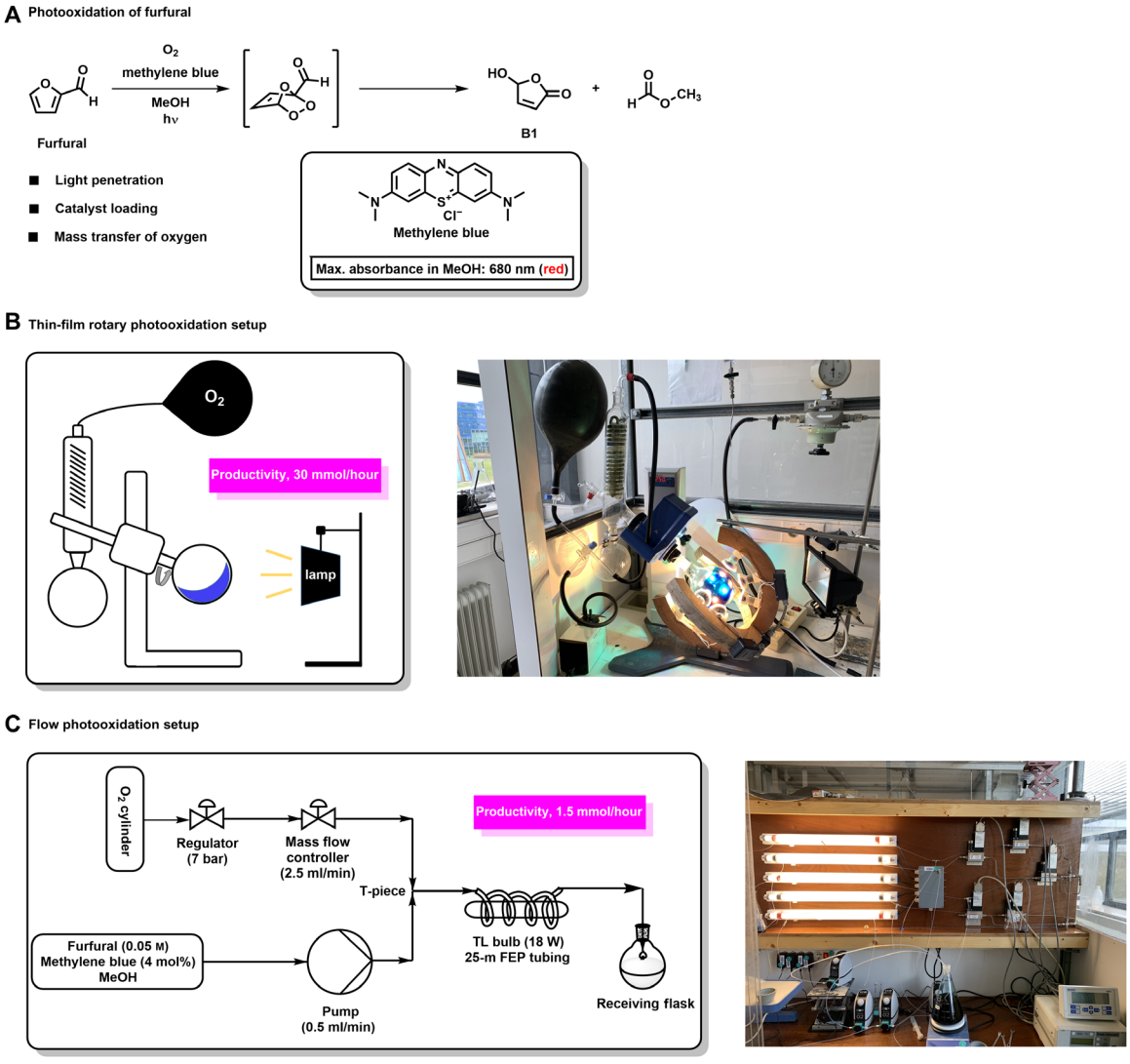

Fig. 2. Upscaling of the photooxidation of furfural. (**A**) Reaction of furfural with singlet oxygen catalyzed by the photosensitizer methylene blue (shown in box) yielding hydroxybutenolide **B1**. (**B**) Rotary evaporator photoreactor setup scheme (left); picture of rotary thin-film system in operation (right) using a 10 × 80–W white light LED setup (see the Supplementary Materials pages S5 and S6 for experimental details and photoreactor setup, and table S1 for full optimization details). (**C**) Flow photooxidation setup scheme (left) and picture of five parallel flow systems in operation (right). A detailed description of the experimental setup and optimization can be found in fig. S4 and table S2. Photo credit (B and C): J. G. H. Hermens, University of Groningen.

examples include linear and branched alcohols and the natural product (−)-menthol (Fig. 1B). It should be noted that the entire synthetic route from biomass to alkoxybutenolide monomers is environmentally benign as it meets multiple requirements of the Twelve Principles of Green Chemistry. An analysis of key features of this process against the Principles of Green Chemistry is presented in Table 1 (*26*).

Polymerization and copolymerization

Next, we explored the radical (co)polymerization of methoxybutenolide **B2** in solution. Initially, various conditions and reaction partners were examined to establish an optimal polymerization procedure (Fig. 3A). As the reactivity of the butenolide is reduced compared with common acrylate esters as a result of the presence of an internal alkene in **B2**, slower kinetics were observed in radical polymerizations carried out under standard conditions using butyl acetate [boiling point (bp.), 126°C] as solvent and Trigonox 42S ($t_{1/2}$: 1 hour at 114°C) as a radical initiator. Homopolymerization of methoxybutenolide **B2** was achieved in 3.5 hours (34% conversion), which could be increased to 53% upon changing the solvent to 1-methoxy-2-propanol (bp., 120°C) (Fig. 3B, column 1; see also table S3). Protic solvents tend to show an increased rate of polymerization mainly caused by hydrogen bonding to the carbonyl moiety (*37*), but also chain transfer to monomer could play a role, both contributing to an increase in conversion (*38*, *39*).

Similar results were obtained for homopolymerizations of alkoxybutenolides **B3** to **B5** (Fig. 3B, column 1). Longer reaction times or addition of extra radical initiator did not affect the outcome pointing to inhibited conversion during the later stages of the homopolymerization process (see also Figs. 5A and Fig. 6, vide infra).

Table 1. Justification of the principles of green chemistry. Relevant Principles of Green Chemistry and analysis for the synthesis of alkoxybutenolide monomers from furfural.

Principles of Green Chemistry	Justification
Less hazardous chemical synthesis	In the synthesis, starting from the platform chemical furfural, benign solvents (methanol and toluene) are used for the preparation of alkoxybutenolides. As vacuum distillation is used as the purification method, no other environmentally hazardous solvents are used.
Design for energy efficiency	The oxidation of furfural is performed photochemically (visible light) at ambient temperature. Scalable photooxidation procedures with energy-efficient lamps (TL and LED) have been designed.
Use of renewable feedstocks	Furfural, a platform chemical derived from the acid-mediated dehydration of lignocellulose (H_2O as waste), is used as sole starting material for the synthesis of alkoxybutenolides (*45*, *46*).
Reduce derivatives	The hemiacetal moiety in hydroxybutenolide **B1** allows facile derivatization toward alkoxybutenolides without the use of protecting/activation groups.
Catalysis	The oxidation of furfural is photocatalytic using molecular oxygen, preventing the use of stoichiometric amounts of oxidants.
Inherently safer chemistry for accident prevention	The flow reactor designed for the upscaling of the photooxidation of furfural allows a safer handling of reactive substrates (pressurized oxygen) or intermediates (endoperoxide) as low concentrations, and no accumulation is present in flow (*30*).

Moving forward to the screening of various reaction partners for copolymerization, copolymerization of **B2** with butyl acrylate or styrene, within short reaction times, provided mainly the respective homopolymers with only traces of copolymer formed. This observation reflects the mismatch in reactivity of the monomers. In sharp contrast, 1:1 copolymerization of **B2** with the less reactive vinyl ester and vinyl ether monomers, i.e., vinyl neodecanoate (VeoVa-10) and dodecyl vinyl ether, resulted in excellent conversions of 99% (2 hours) and 95% (50 min), respectively (Fig. 3B, row 1). However, the copolymerization of **B2** with di(ethylene glycol) divinyl ether (DVE) showed a maximum conversion of 69%. In this transformation of **B2** and DVE, an insoluble white material was formed after 6 min, strongly indicating the formation of a polymer network. Similar conversions were achieved for homo- and copolymerizations of **B3** to **B5** with VeoVa-10, dodecyl vinyl ether, and DVE, showing no unfavorable effect upon increasing the size of the alkoxy substituent (Fig. 3B, rows 2 to 4).

From an industrial and practical perspective, it is important to determine monomer conversion in time and obtain detailed polymerization kinetics. Initially, the reaction kinetics of the copolymerization of butenolide **B2** and VeoVa-10 (2.15 M) at 120°C were studied by following the consumption of the individual monomers over a 2-hour period using Raman spectroscopy. Samples were taken at various points during the reaction and flash frozen at −18°C to stop the polymerization. It revealed a rate constant $k_{obs} = 7.4{\cdot}10^{-4}$ s^{-1} and >99% conversion in 2 hours. As we were facing substantial overlap of the Raman bands of dodecyl vinyl ether and the butenolides, the reaction kinetics of the copolymerizations of **B2** to **B5** with VeoVa-10, dodecyl vinyl ether, and di(ethylene glycol) DVE were followed by ^{1}H nuclear magnetic resonance (NMR) spectroscopy using 1,3,5-trimethoxybenzene as an internal standard. The data for the copolymerization of **B2** with VeoVa-10, obtained by ^{1}H NMR spectroscopy, are shown in Fig. 4. This clearly demonstrates 1:1 incorporation of both monomers in an alternating copolymer (Fig. 4C) and complete conversion of methoxybutenolide **B2** and VeoVa-10 (Fig. 4D). It should be noted that higher rate constants were observed for the copolymerization of **B2** with vinyl ethers dodecyl vinyl ether and di(ethylene glycol) DVE compared to the copolymerization of **B2** with vinyl ester VeoVa-10. Gratifyingly, similar reactivity in homopolymerizations (Fig. 5A) and copolymerizations (Fig. 5, B to D) was observed for all the alkoxybutenolides, and again, higher rates were found for the reactions with vinyl ethers than with vinyl esters.

It was also observed that the copolymerization of butenolides **B3** and **B5** with VeoVa-10 shows inhibition at higher conversion, albeit only observable at >92% conversion, reminiscent of the homopolymerizations of butenolides **B2** to **B5**. Depending on the (co)monomer, upon extended radical polymerization, a competing radical process is taking place. We envisioned that the increase in polymer concentration could influence the propagation of the remaining monomers. To examine this in more detail, the copolymerization of menthyloxybutenolide **B5** with VeoVa-10 was followed in time, and presynthesized menthyloxybutenolide–VeoVa-10–copolymer **MP2** (1 ml of 2.15 M solution in 1-methoxy-2-propanol) was added at $t = 40$ min. This induced immediate inhibition of the propagation at this stage (74% conversion) with a similar rate constant as was obtained for the initial inhibited copolymerization at 92% conversion (Fig. 6). In brief, we propose that inhibition of the radical propagation step in the polymerization at low rates (at the stage of high monomer conversion) is the result of H-abstraction by the propagating radical from the acetal position in the lactone moiety, generating a captodative stabilized radical (*40*, *41*).

Focusing on the properties of the polymers, the molecular weight distribution and glass transition temperatures were analyzed for the copolymers of **B2** to **B5** with VeoVa-10 and dodecyl vinyl ether to reveal the effect of the alkoxy substituents on the quality of the polymers. The polymers were subjected to gel permeation chromatography (GPC) using a polystyrene-calibrated column. The molecular weight distribution of the copolymers of **B2** to **B5** with VeoVa-10 and dodecyl vinyl ether is typically in the range M_w 2800 to 3300 g/mol and 4300 to 4900 g/mol, respectively (Table 2). As the differences in molecular weights of the butenolide polymers are small, it is evident the alkoxy substituents have little impact on the polymerization process. As a comparison, the homopolymer and copolymer (with VeoVa-10) of butyl acrylate were subjected to GPC, and higher molecular weights are found M_w 10,000 to 15,000 g/mol. Glass transition temperature (T_g) data, however, indicate large differences between the different butenolide polymers, showing that the properties of the (co)polymers can be fine-tuned through the choice of alcohol

A

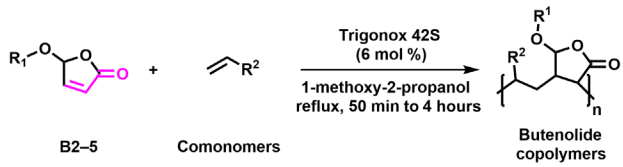

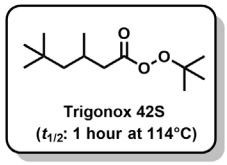

B

	Monomer	Conversion (co)polymerization (%) Homo-polymerization	VeoVa-10	Dodecyl vinyl ether	Di(ethyleneglycol) divinyl ether
B2		53	99	95	69[a]
B3	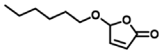	51	92	>99	>99
B4	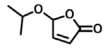	37	96	>99	91[a]
B5	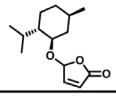	30	92	>99	>99

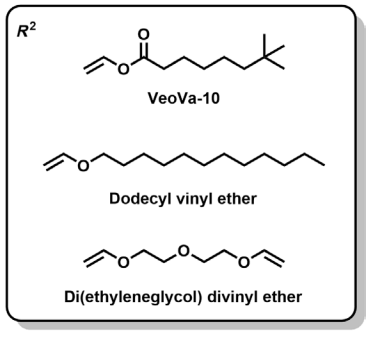

Fig. 3. Homo- and copolymerization of alkoxybutenolide. (**A**) Reaction scheme, structures of (co)monomers, and conversions. General (co)polymerization reaction, reaction conditions: butenolides-comonomers (1:1 ratio), Trigonox 42S (6 mol %), 2.15 M in 1-methoxy-2-propanol, reflux, 50 min to 4 hours. (**B**) Substrate conversion of alkoxybutenolides, homopolymerization (column 1), and copolymerization (columns 2 to 4); butenolides-comonomers (1:1 ratio), in the case of di(ethylene glycol) divinyl ether 1:0.5 ratio. (A) Maximum conversion obtained for copolymerization of **B2**, DVE and **B4**, DVE due to formation of insoluble material. For a complete overview of co-polymerization reactions, see table S38.

in the alkoxybutenolide monomer. The lowest glass transition temperatures are obtained for hexyloxybutenolide polymers **HP2** and **HP3** as, generally, the T_g decreases with increased flexibility of the monomer (*42*). In contrast, the more rigid structure of menthol increases the T_g and accounts for the highest values obtained. The substitution of the hexyl chain for menthol in the case of **HP3** and **MP3** results in a difference of 88°C in T_g.

Coating formation

Having established the key features [(co-)polymerization rates and polymer properties] of the previously unknown alkoxybutenolide monomers in (co-)polymerization, we proceeded to the formation of surface coatings. The process we used for coating formation is shown in Fig. 7. A variety of coatings was obtained by polymerization of monomers **B2** to **B5** in the presence of di(ethylene glycol) DVE as cross-linker using ultraviolet (UV) curing as the optimal way for preparing the coatings on surfaces. In all cases, solvent-free radiation-cured coatings were obtained within short curing times. Typically, neat mixtures of alkoxybutenolides, DVE, and Omnirad 819 as radical photoinitiator were applied on glass surfaces (Fig. 7). After 5 min of irradiation (λ_{irr} = 395 nm), uniform coatings were obtained, and an optimal film thickness of the coatings of 100 μm was established.

Clear, hard, and transparent coatings were obtained as illustrated for the methoxybutenolide-derived coating **BP4** on glass shown in Fig. 8A. To determine the properties of these novel bio-based materials, we subjected the coatings to standardized spot tests to reveal the resistances against water and solvent (*43*, *44*). The Persoz hardness test was used to establish the hardness, and the glass transition temperatures and cross-link densities were measured by dynamic mechanical thermal analysis (DMTA). To our delight, all butenolide coatings showed excellent water and solvent resistance using standard spot tests, considering the methoxy coating (**BP4**), isopropoxy coating (**IP4**), and menthyloxy coating (**MP4**) only showed very minor discoloring (Fig. 8B). The coating performance data as summarized in Fig. 8E clearly show that the alkyl substituent of the alkoxybutenolide unit has a significant influence on their properties. Typically, these coatings present different properties in terms of hardness, as a change in branching or flexibility in the side chain (from methyl to isopropyl to hexyl) reduces the hardness of the coating. On the contrary, because of the more rigid structure of menthol, a high hardness is obtained for **MP4**.

We showed earlier, on the basis of the reaction kinetic data and GPC analysis, that the various butenolide monomers **B2** to **B5** follow similar reactivity, and variations in molecular weight with different chain lengths are small. This supports the notion that the differences in coating properties are mainly attributed to the nature of the alkoxy substituents. An inherent property directly related to the different values of hardness is the ability to coat distinct surfaces. The butenolide coatings **BP4**, **IP4**, and **MP4** are excellent candidates for glass surfaces (Fig. 8A). On the contrary, the softer, more hydrophobic, hexyloxybutenolide coating **HP4** not only is a good candidate for glass surfaces (Fig. 8C) but also performs excellent on polypropylene surfaces as the coating does not break upon UV curing (Fig. 8D).

The cross-link density and the glass transition temperatures were determined via DMTA (Fig. 8E). Because the strain and stress of the coatings were measured on polypropylene surfaces, VeoVa-10 was added to increase the hydrophobicity of the coatings **BP4**, **IP4**, and **MP4**, while simultaneously lowering the hardness, to properly form a nonbrittle uniform film of these coatings on polypropylene. Therefore, the measured T_g and cross-link density are lower than the actual T_g and cross-link density of the coatings without the addition of VeoVa-10 on glass. The measured glass transition temperatures follow the same trend observed before, i.e., decreasing T_g upon increasing flexibility.

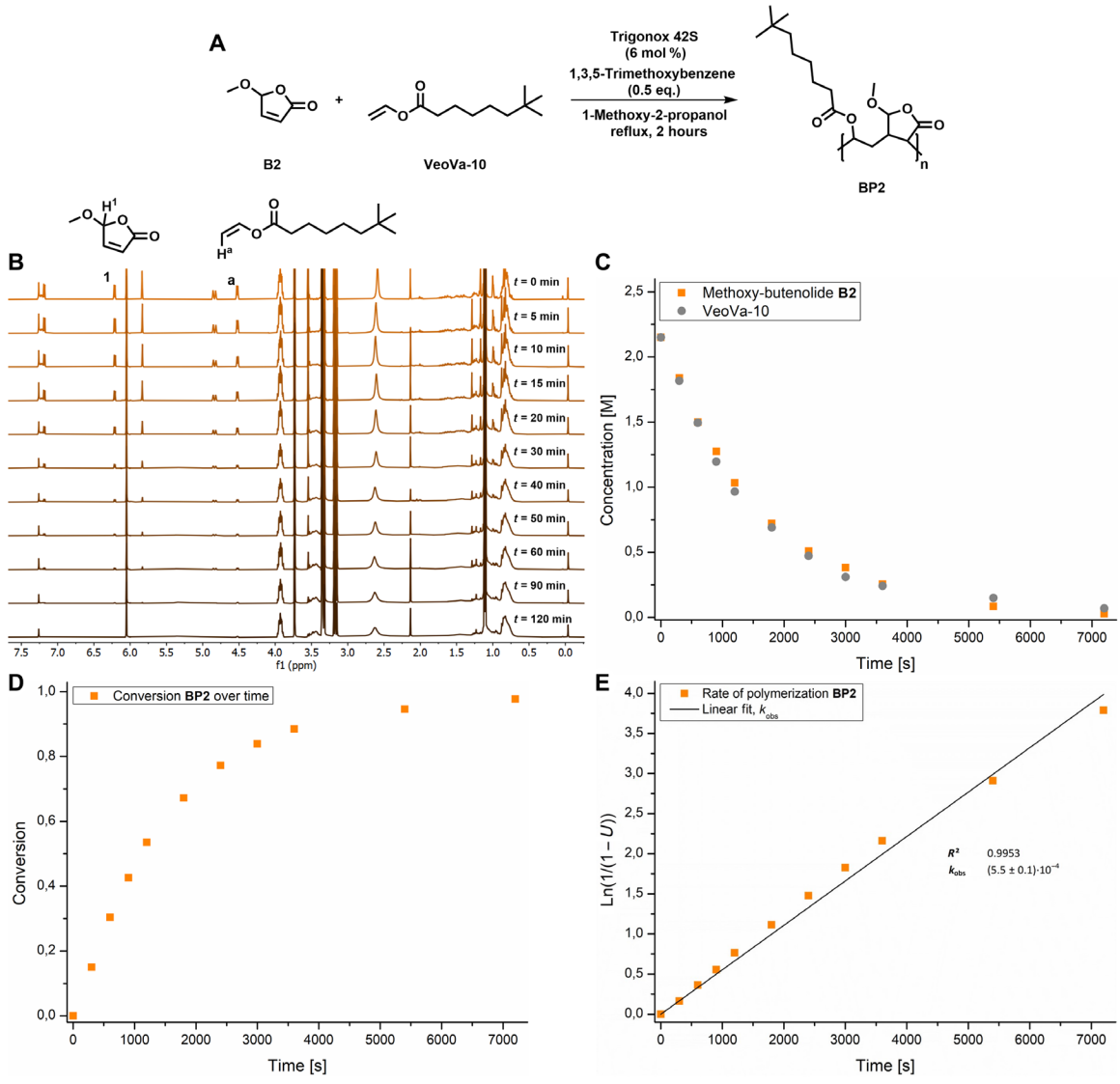

Fig. 4. Reaction kinetics of the copolymerization of B2 with VeoVa-10. (**A**) Copolymerization of methoxybutenolide **B2** with VeoVa-10 (1:1 ratio), followed by ^{1}H NMR spectroscopy using 1,3,5-trimethoxybenzene (0.5 eq.) as internal standard, reaction conditions: Trigonox 42S (6 mol %), 2.15 M in 1-methoxy-2-propanol, reflux, 2 hours. (**B**) ^{1}H NMR signals over time by taking samples and flash freezing (−18°C) them at certain timestamps. (**C**) Concentration of monomers over time during the copolymerization of **B2** with VeoVa-10. (**D**) Conversion of polymer **BP2** over time. (**E**) Rate of copolymerization of **B2** and VeoVa-10. (For full kinetic analysis of all copolymerizations, see also figs. S10 to S143, tables S4 to S38, and the Supplementary Materials pages S30 to S210.). ppm, parts per million.

DISCUSSION

On the basis of the data of our coatings shown in Fig. 8, it should be emphasized that their properties are comparable to common coatings based on acrylates. As demonstrated here for both glass and plastic materials, uniform robust thin-film coatings are readily obtained, and above all, the properties (hardness and polarity) are easily tunable for different surface applications. The properties of these coatings, in terms of resistance and hardness, are comparable or even better with those of current industrial ultraviolet A (UV-A) light curable clear coatings for car furnishes (*44*).

In conclusion, we have demonstrated a previously undiscovered sustainable route to coatings based on abundant green starting material, common alcohols, and molecular oxygen using a photochemical process applying visible light. This study shows that starting from biomass-derived furfural, by applying photooxidation in a flow system, alkoxybutenolide monomers are accessible as alternatives for common acrylates. The formation of coatings with excellent solvent resistance and hardness, comparable to current industrial coatings, as well as tunable properties for application on different surfaces illustrates a viable green route to materials abundantly used in modern society.

MATERIALS AND METHODS

Photooxidation of furfural (immersion well setup)

To the large photooxygenation setup shown in fig. S2, freshly distilled (50°C, 1.5×10^{-2} mbar) furfural (50.0 g, 0.52 mol, 1 eq.) dissolved in 500 ml of oxygen-enriched methanol was added. Methylene blue

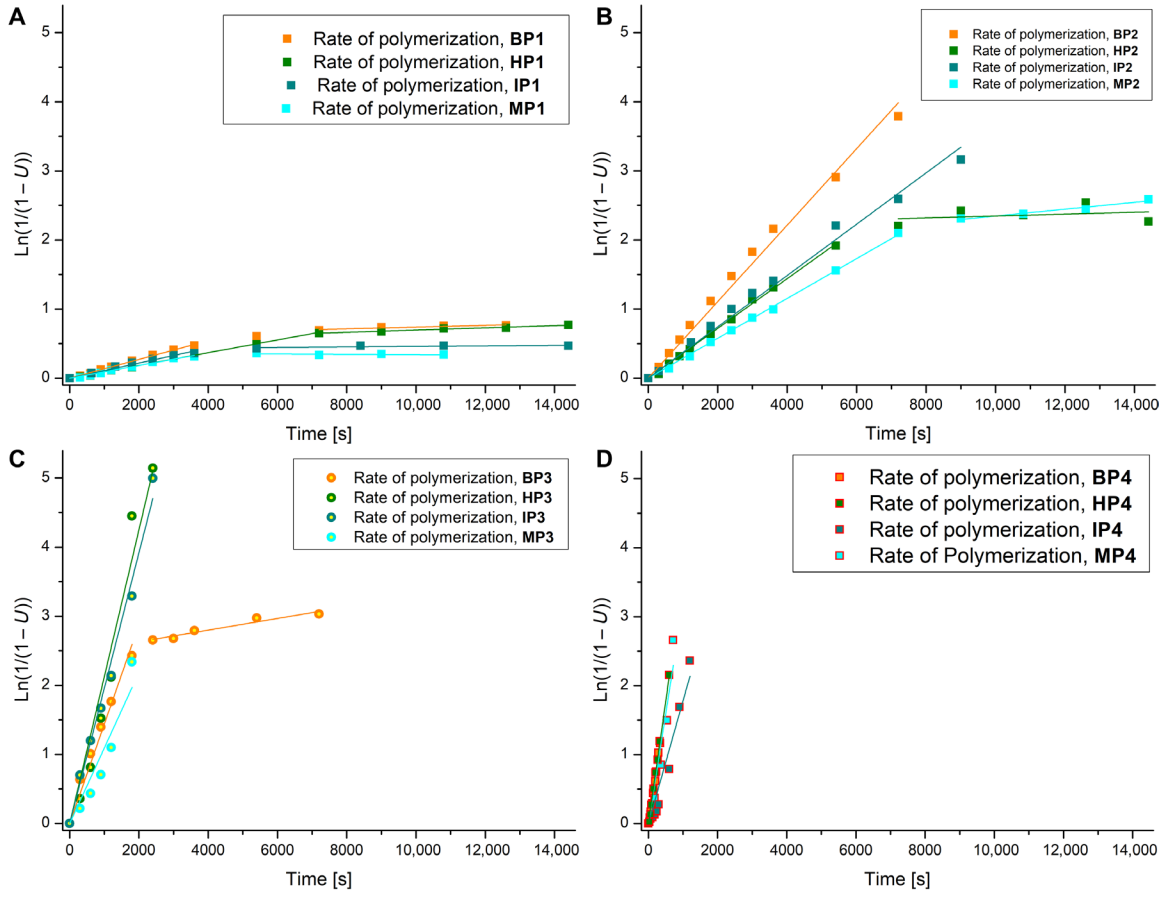

Fig. 5. Rate of (co)polymerization B2 to B5 with comonomer. (Homopolymerization of **B2** to **B5** (2 eq.) and copolymerizations of **B2** to **B5** with comonomers VeoVa-10 (1:1 ratio), dodecyl vinyl ether (1:1 ratio), and di(ethylene glycol) DVE (1:0.5 ratio), reaction conditions: Trigonox 42S (6 mol %) (3 mol % in case of homopolymerization), 2.15 M in 1-methoxy-2-propanol (4.3 M in case of homopolymerization), reflux, 6 min to 4 hours. Rate of polymerization [ln(1/(1 − *U*)] as a function of *t* where *U* = conversion of polymer. (**A**) Rates of homopolymerization methoxybutenolide (**BP1**), hexyloxybutenolide (**HP1**), isopropoxybutenolide (**IP1**), and menthyloxybutenolide (**MP1**). (**B**) Rate of copolymerization of VeoVa-10 with methoxybutenolide (**BP2**), hexyloxybutenolide (**HP2**), isopropoxybutenolide (**IP2**), and menthyloxybutenolide (**MP2**). (**C**) Rates of copolymerization of dodecyl vinyl ether with methoxybutenolide (**BP3**), hexyloxybutenolide (**HP3**), isopropoxybutenolide (**IP3**), and menthyloxybutenolide (**MP3**). (**D**) Rate of copolymerization of di(ethylene glycol) DVE with methoxybutenolide (**BP4**), hexyloxybutenolide (**HP4**), isopropoxybutenolide (**IP4**), and menthyloxybutenolidebutenolide (**MP4**) (see also table S38).

[10 mg, 0.032 mmol, 0.005 mole percent (mol %)] was added to the reaction mixture. An oxygen line was connected to the bottom inlet of the setup, and oxygen was bubbled through the solution with a controlled flow. Red light-emitting diodes (LEDs) (150 lm, λ = 680 nm) were inserted in the glass tube, and the glass tube was put in the setup. The resulting mixture was bubbled with oxygen for 120 hours while irradiated by red light. The reaction was followed by ^{1}H NMR until all furfural was consumed. The solvent was evaporated after under reduced pressure. The obtained oil solidified upon standing. The product 5-hydroxy-2(5*H*)-furanone **B1** could be used without further purification. Removal of the photosensitizer was done by filtration in diethyl ether over silica and charcoal. After evaporation, the compound was recrystallized at −78°C to form the product 5-hydroxy-2(5*H*)-furanone **B1** as an off-white crystalline solid (52.1 g, 0.52 mol, quantitative).

Photooxidation of furfural (rotary evaporator setup)

A solution of freshly distilled (50°C, 1.5×10^{-2} mbar) furfural (1.0 g, 10 mmol, 1 eq.) and methylene blue (17 mg, 52 μmol, 0.5 mol %) in 10 ml of oxygen-enriched methanol was prepared in a 1000-ml round-bottom flask. The mixture was put under an oxygen atmosphere in a standard laboratory rotary evaporator (175 rpm) and irradiated by 8 × 80–W LED lamps for 20 min. The light sources were placed at a distance of 5 cm from the flask (see fig. S3). The solvent was evaporated after under reduced pressure. The obtained oil solidified upon standing. The product 5-hydroxy-2(5*H*)-furanone **B1** could be used without further purification. Removal of the photosensitizer was done by filtration in diethyl ether over silica and charcoal. After evaporation, the compound was recrystallized at −78°C to form the product 5-hydroxy-2(5*H*)-furanone **B1** as an off-white crystalline solid (1.0 g, 10 mmol, quantitative).

Photooxidation of furfural (flow reactor setup)

A solution of freshly distilled (50°C, 1.5×10^{-2} mbar) furfural (10.0 g, 104 mmol, 1 eq.) and methylene blue (128 mg, 0.4 mmol, 4 mol %) in 2000 ml of oxygen-enriched methanol was prepared in a 2-liter Erlenmeyer flask. The reaction mixture was stirred for 30 min before the lines of the dosing pumps were put in the solution. The

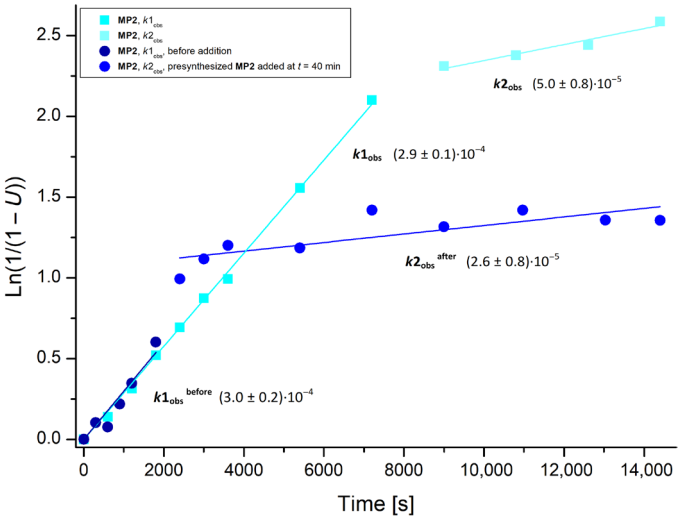

Fig. 6. Inhibition after the addition of presynthesized copolymer MP2. Reaction conditions: Trigonox 42S (6 mol %), 2.15 M in 1-methoxy-2-propanol, reflux, 4 hours. Inhibited polymerization of menthyloxybutenolide **B5** with VeoVa-10 (1:1 ratio, cyan line) at 92% conversion, t = 9000 s. Polymerization of menthyloxybutenolide **B5** with VeoVa-10 (1:1 ratio, dark blue line) until t = 1800 s. Inhibited polymerization of menthyloxybutenolide **B5** with VeoVa-10 after the addition of presynthesized menthyloxybutenolide–VeoVa-10–copolymer **MP2** (1 ml of 2.15 M solution in 1-methoxy-2-propanol, 92% conversion) (1:1 ratio, blue line) at t = 2400 s. Similar reaction rates are obtained, $k2_{obs}^{before} = 5.0 \cdot 10^{-5}\ s^{-1}$ and $k2_{obs}^{after} = 2.6 \cdot 10^{-5}\ s^{-1}$, for the inhibited polymerization at t = 9000 s (cyan line) and the induced inhibited polymerization at t = 2400 s (blue line). For further elucidation of this polymerization behavior, control experiments, and kinetic data and analysis, see the Supplementary Materials pages S179 to S209.

dosing pumps were primed with the solution and were set to a flow of 0.5 ml/min. The reaction mixture was pumped through the reaction line together with a flow (2.5 ml/min) of oxygen and irradiated by a TL bulb. The resulting reaction mixture was received and transferred to a round-bottom flask. The solvent was evaporated under reduced pressure, and the crude blue oil was distilled to remove unreacted furfural (50°C, 1.5 × 10^{-2} mbar). The obtained blue oil solidified upon standing. The product 5-hydroxy-2(5*H*)-furanone **B1** could be used without further purification. Removal of the photosensitizer was done by filtration in diethyl ether over silica and charcoal. After evaporation, the compound was recrystallized at −78°C to form the product 5-hydroxy-2(5*H*)-furanone **B1** as an off-white crystalline solid (10.2 g, 102 mmol, 98%).

Synthesis of methoxybutenolide B2

5-Hydroxy-2(5*H*)-furanone **B1** (100.0 g, 1 mol) was dissolved in 500 ml of dry methanol and heated at reflux for 20 hours. The conversion was followed by ^{1}H NMR until all 5-hydroxy-2(5*H*)-furanone **B1** was consumed. The solvent was evaporated under reduced pressure, and the crude was distilled under reduced pressure (70°C, 1.0 × 10^{-2} mbar), yielding 5-methoxy-2(5*H*)-furanone **B2** (86.5 g, 0.76 mol, 76%) as a slightly yellow oil.

Synthesis of hexyloxybutenolide B3

5-Hydroxy-2(5*H*)-furanone **B1** (62.0 g, 0.62 mol, 1 eq.) and anhydrous hexanol (104.5 g, 1.02 mol, 1.65 eq.) were dissolved in 180 ml of toluene and heated at reflux under azeotropic removal of water for 20 hours. The solvent was evaporated under reduced pressure, and the crude was fractionally distilled under reduced pressure (100°C,

Table 2. Properties of butenolide polymers. Polymer properties of alkoxybutenolide-based polymers **BP2**, **BP3**, **HP2**, **HP3**, **IP2**, **IP3**, **MP2**, and **MP3** and butyl acrylate polymers homopolymer **BAP1** and copolymer with VeoVa-10 **BAP2** for comparison; molecular weights, length, and glass transition temperature (T_g).

Polymer*	Monomer 1	Monomer 2	M_n (g/mol)	M_w (g/mol)	D†	n‡	T_g (°C)
BP2		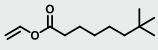	**1165**	**2,789**	**2.39**	**8.93**	**12**
BP3		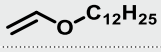	**1611**	**4,882**	**3.03**	**14.69**	**−62**
HP2	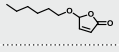	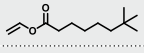	**1242**	**3,264**	**2.63**	**8.54**	**−27**
HP3	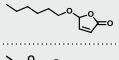	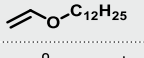	**1548**	**4,587**	**2.96**	**11.57**	**−72**
IP2		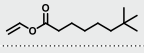	**1572**	**3,174**	**2.02**	**9.32**	**12**
IP3		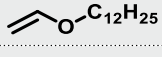	**1764**	**4,295**	**2.43**	**12.12**	**−67**
MP2		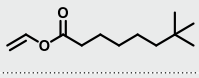	**1151**	**3,101**	**2.69**	**7.11**	**24**
MP3		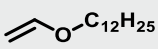	**1584**	**4,711**	**2.97**	**10.46**	**16**
BAP1		/	**4022**	**15,860**	**3.94**	**123.72**	**−39**
BAP2	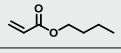	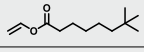	**2806**	**10,766**	**3.84**	**33.00**	**−50**

*Reaction conditions: 1:1 ratio of monomers, Trigonox 42S (6 mol %), 2.15 M in 1-methoxy-2-propanol, reflux, 10 min to 4 hours. †Polydispersity (D) is calculated by dividing M_w by M_n. ‡Average amount of units in the polymer chain (n) is calculated through dividing number average molecular weight (M_n) by average mass of unit (mass monomer 1 + mass monomer 2).

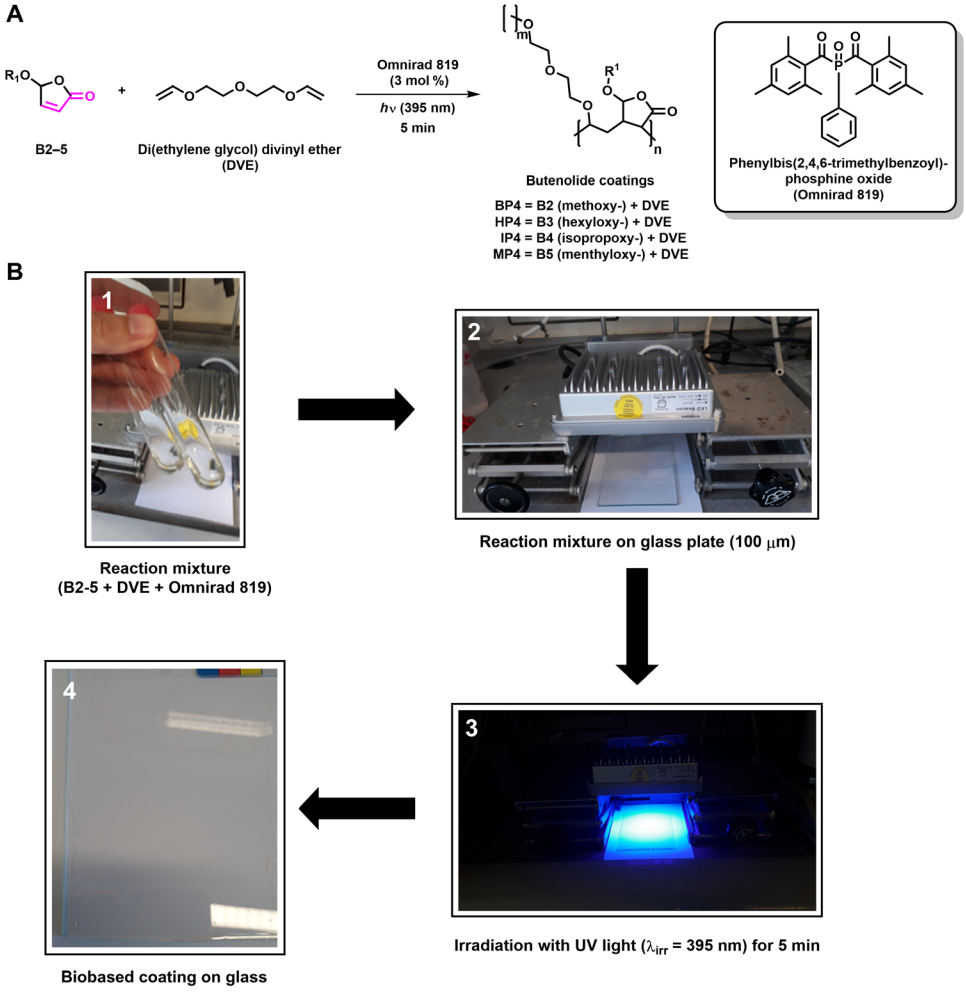

Fig. 7. Coating formation of alkoxybutenolides. (**A**) General cross-linking reaction of alkoxybutenolides (1 eq.) with DVE (0.5 eq.), Omnirad 819 (3 mol %) as radical initiator and UV light (λ_{irr} = 395 nm, 5 min) as trigger. Coating coding: **BP4** = **B2** (methoxy-) + DVE, **HP4** = **B3** (hexyloxy-) + DVE, **IP4** = **B4** (isopropoxy-) + DVE, **MP4** = **B5** (menthyloxy-) + DVE. (**B**) Through (1) mixing alkoxybutenolide **B2** to **B5** with DVE and Omnirad 819 until a homogeneous mixture is obtained, (2) applying the mixture uniformly on a glass plate (100 μm) using a Byk applicator, and (3) irradiating the glass plate for 5 min with UV light (λ_{irr} = 395 nm), (4) a hard transparent butenolide-based coating is formed. For figures of butenolide coatings on glass plates, see figs. S167 to S172. Photo credit (B): R. van Gemert, AkzoNobel Car Refinishes BV.

1.0×10^{-2} mbar), yielding a yellow oil. The yellow oil was further purified by column chromatography (silica gel, *n*-pentane:ethyl acetate/90:10), yielding 5-hexyloxy-2(5*H*)-furanone **B3** (60.4 g, 0.33 mol, 53%) as a slightly yellow oil.

Synthesis of isopropoxybutenolide B4

5-Hydroxy-2(5*H*)-furanone **B1** (70.0 g, 0.7 mol, 1 eq.) was dissolved in 250 ml of anhydrous 2-propanol and heated at reflux for 20 hours. The solvent was evaporated under reduced pressure, and the crude was fractionally distilled under reduced pressure (90°C, 1.4×10^{-2} mbar), yielding a yellow oil. The yellow oil was further purified by column chromatography (silica gel, *n*-pentane:ethyl acetate/90:10), yielding 5-isopropoxy-2(5*H*)-furanone **B4** (44.6 g, 0.31 mol, 45%) as a colorless oil.

Synthesis of menthyloxybutenolide B5

5-Hydroxy-2(5*H*)-furanone **B1** (60.0 g, 0.6 mol, 1 eq.), (−)-menthol (101.3 g, 0.65 mol, 1.08 eq.), and catalytic amounts of *p*-TsOH (0.57 g, 3 mmol, 0.005 eq.) were dissolved in 175 ml of toluene and heated at reflux under azeotropic removal of water for 20 hours. The solvent was evaporated under reduced pressure, and the crude was fractionally distilled under reduced pressure (120°C, 1.4×10^{-2} mbar), yielding a yellow oil. An impurity of unsaturated aldehyde was removed from the residue by dissolving the crude yellow oil in an ethereal solution of diethyl ether and a saturated solution of $NaHSO_3$ for 30 min. The water layer was extracted three times with diethylether. After combining all organic fractions, the organic layer was washed three times with H_2O, dried over $MgSO_4$, and filtered, and the solvent was evaporated under reduced pressure, yielding a slightly yellow oil that solidified upon standing as a white solid (58.6 g, 0.25 mol, 41%) consisting of two diastereomers (ratio 58:43). Recrystallization from *n*-heptane and washing with cold (−18°C) *n*-heptane yielded diastereomerically pure 5-menthyloxy-2(5*H*)-furanone **B5** as was determined by ^{1}H NMR and ^{13}C NMR spectroscopy. Through combination of the mother liquors and repeating this step, multiple crops of diastereomerically pure white crystalline product were obtained.

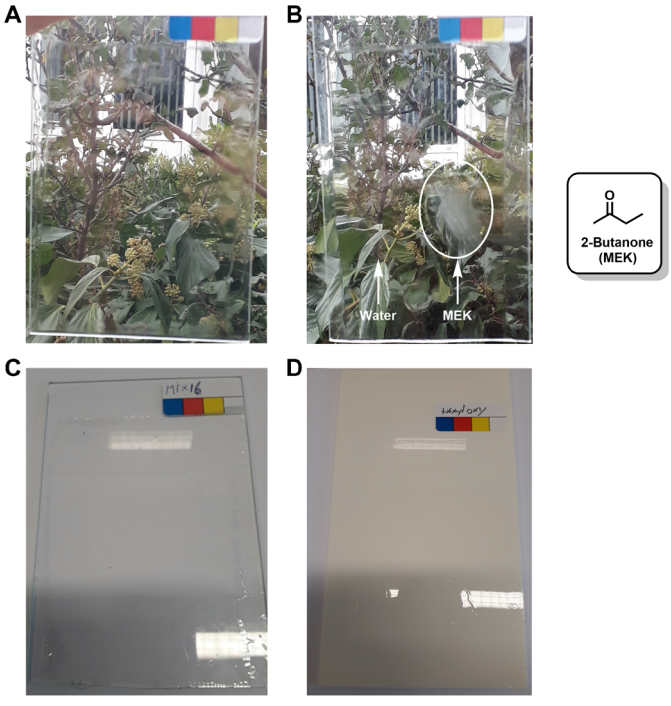

E

Polymer	Monomer 1	Dry film thickness (μm)	Water resistance (0–5)[a]	MEK resistance (0–5)[a]	Hardness (oscillations)	Glass transition temperature (°C)
BP4		120	5	3	249	ND
BP4		100	5	4	285	156[c]
HP4	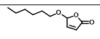	100	5	5	145	86
IP4		100	5	4	241	95[c]
MP4[b]		100	5	4	261	108[c]

Fig. 8. Butenolide coatings and properties. Coating formation conditions: Alkoxybutenolide **B2** to **B5** (1 eq.), di(ethylene glycol) DVE (0.5 eq.) Omnirad 819 (3 mol %), UV light (λ_{irr} = 395 nm), 5 min. (**A**) Clear, uniform, and hard methoxybutenolide coating **BP4** on glass (100 μm). (**B**) Methoxybutenolide coating **BP4** subjected to standardized spot tests, droplet of water removed after 1 hour, droplet of 2-butanone [methyl ethyl ketone (MEK)] removed after 1 min. Water has no effect on coating, resulting in no visible defects. MEK has a minor effect on coating, resulting in very slight discoloring. (**C**) Clear, uniform, and hard hexyloxybutenolide coating **HP4** on glass (100 μm). (**D**) Clear, uniform, and hard hexyloxybutenolide coating **HP4** on polypropylene (100 μm). Photo credit (A to D): R. van Gemert, AkzoNobel Car Refinishes BV. (**E**) Summary of the properties of the various alkoxybutenolide coatings. [a]Water/MEK resistance, 0 = damaged coating, 5 = no damage, general procedure in the Supplementary Materials page S240. [b]23 weight % of butyl acetate was added to dissolve the monomers. [c]VeoVa-10 added for increasing hydrophobicity to coat on polypropylene, butenolide/DVE/VeoVA-10—2/0.7/0.6 equiv. ND, not determined (Supplementary Materials pages S240–S242). For all coatings on glass plates, see the Supplementary Materials pages S234–S239; for DMTA, see the Supplementary Materials pages S241–S247; and for BP4, IP4, and MP4 coated on polypropylene, see figs. S168 to S171.

General procedure (co)polymerization reaction

To a 4-ml vial with screwcap with septum, alkoxybutenolide **B2** to **B5** (2 mmol, 1 eq.), the corresponding comonomer (2 mmol, 1 eq.), and 1-methoxy-2-propanol (1 ml) were added. 1,3,5-Trimethoxybenzene (181 mg, 1 mmol, 0.5 eq.) was added as an internal standard for ^{1}H NMR measurements. The mixture was heated to 120°C, and Trigonox 42S (0.03 mg, 0.033 μl, 6 mol %, 0.06 eq.) was added as an initiator. The mixture was refluxed for 10 min to 4 hours, depending on the desired polymer. At regular intervals, a sample of 50 μl was taken from the mixture and put in a small vial, which was flash frozen (−18°C) to stop polymerization. The reaction kinetics were followed, and the conversion was determined by ^{1}H NMR spectroscopy. In case of homopolymerization, the concentration of the monomer was doubled to account for the net concentration of alkenes in the reaction mixture.

General procedure UV curing of coatings

To a 5-ml vial, alkoxybutenolide **B2** to **B5** (2 mmol, 1 eq.), di(ethylene glycol) DVE (1 mmol, 0.5 eq.), and phenylbis(2,4,6-trimethylbenzoyl) phosphine oxide (Omnirad 819, 60 μmol, 3 mol %) were added and stirred until the reaction mixture became homogeneous. The mixture was applied on a glass surface, and the surface (10 × 20 cm) was coated with a Byk applicator (100- to 150-μm thickness). The glass surface was irradiated with UV-A light (LED beacon ROHS CE IP65, 12 LEDS, WW, 22°C, λ_{irr} = 395 nm) at 10-cm distance for 5 min (total irradiance of 4.5 mW/cm^2).

SUPPLEMENTARY MATERIALS

Supplementary material for this article is available at http://advances.sciencemag.org/cgi/content/full/6/51/eabe0026/DC1

REFERENCES AND NOTES

1. R. Lambourne, T. A. Strivens, *Paint and Surface Coatings* (Woodhead Publishing, Cambridge, ed. 2, 1999).
2. T. Ohara, T. Sato, N. Shimizu, G. Prescher, H. Schwind, O. Weiberg, K. Marten, H. Greim, *Acrylic Acid and Derivatives. Ullmann's Encyclopedia of Industrial Chemistry* (Wiley, Weinheim, 2011).
3. M. Poliakoff, J. M. Fitzpatrick, T. R. Farren, P. T. Anastas, Green chemistry: Science and politics of change. *Science* **297**, 807–810 (2002).
4. J. B. Zimmerman, P. T. Anastas, H. C. Erythropel, W. Leitner, Designing for a green chemistry future. *Science* **367**, 397–400 (2020).
5. M. Beller, G. Centi, L. Sun, Chemistry future: Priorities and opportunities from the sustainability perspective. *ChemSusChem* **10**, 6–13 (2016).
6. G. Alfke, W. W. Irion, O. S. Neuwirth, *Oil Refining. Ullmann's Encyclopedia of Industrial Chemistry* (Wiley, Weinheim, 2007).
7. A. Niesbach, R. Fuhrmeister, T. Keller, P. Lutze, A. Górak, Esterification of acrylic acid and *n*-butanol in a pilot-scale reactive distillation column—Experimental investigation, model validation, and process analysis. *Ind. Eng. Chem. Res.* **51**, 16444–16456 (2012).
8. W. Leitner, J. Klankermayer, S. Pischinger, H. Pitsch, K. Kohse-Höinghaus, Advanced biofuels and beyond: Chemistry solutions for propulsion and production. *Angew. Chem. Int. Ed.* **56**, 5412–5452 (2017).
9. I. Delidovich, P. J. C. Hausoul, L. Deng, R. Pfützenreuter, M. Rose, R. Palkovits, Alternative monomers based on lignocellulose and their use for polymer production. *Chem. Rev.* **116**, 1540–1599 (2016).
10. J. Langanke, A. Wolf, J. Hofmann, K. Böhm, M. A. Subhani, T. E. Müller, W. Leitner, C. Gürtler, Carbon dioxide (CO_2) as sustainable feedstock for polyurethane production. *Green Chem.* **16**, 1865–1870 (2014).
11. S. Schmidt, B. S. Ritter, D. Kratzert, B. Bruchmann, R. Mülhaupt, Isocyanate-free route to poly(carbohydrate–urethane) thermosets and 100% bio-based coatings derived from glycerol feedstock. *Macromolecules* **49**, 7268–7276 (2016).
12. M. Nielsen, H. Junge, A. Kammer, M. Beller, Towards a green process for bulk-scale synthesis of ethyl acetate: Efficient acceptorless dehydrogenation of ethanol. *Angew. Chem. Int. Ed.* **51**, 5711–5713 (2012).
13. K. Yan, C. Jarvis, J. Gu, Y. Yan, Production and catalytic transformation of levulinic acid: A platform for speciality chemicals and fuels. *Renew. Sustain. Energy Rev.* **51**, 986–997 (2015).
14. G. E. M. Crisenza, P. Melchiorre, Chemistry glows green with photoredox catalysis. *Nat. Commun.* **11**, 803 (2020).
15. S. Tang, Y. Liu, A. Lei, Electrochemical oxidative cross-coupling with hydrogen evolution: A green and sustainable way for bond formation. *Chem* **4**, 27–45 (2018).

16. Y. Y. Birdja, E. Pérez-Gallent, M. C. Figueiredo, A. J. Göttle, F. Calle-Vallejo, M. T. M. Koper, Advances and challenges in understanding the electrocatalytic conversion of carbon dioxide to fuels. *Nat. Energy* **4**, 732–745 (2019).
17. R. A. Sheldon, The *E* factor 25 years on: The rise of green chemistry and sustainability. *Green Chem.* **19**, 18–43 (2017).
18. O. Konuray, X. Fernández-Francos, X. Ramis, À. Serra, State of the art in dual-curing acrylate systems. *Polymers* **10**, 178 (2018).
19. F. N. Jones, M. E. Nichols, S. P. Pappas, *Organic Coatings: Science and Technology* (Wiley, Weinheim, ed. 4, 2017), pp. 416–417.
20. P. Li, S. Ma, J. Dai, X. Liu, Y. Jiang, S. Wang, J. Wei, J. Chen, J. Zhu, Itaconic acid as a green alternative to acrylic acid for producing a soybean oil-based thermoset: Synthesis and properties. *ACS Sustainable Chem. Eng.* **5**, 1228–1236 (2017).
21. S. P. Arnaud, E. Andreou, L. V. G. Pereira Köster, T. Robert, Selective synthesis of monoesters of itaconic acid with broad substrate scope: Biobased alternatives to acrylic acid? *ACS Sustainable Chem. Eng.* **8**, 1583–1590 (2020).
22. J. T. Trotta, M. Jin, K. J. Stawiasz, Q. Michaudel, W.-L. Chen, B. P. Fors, Synthesis of methylene butyrolactone polymers from itaconic acid. *J. Polym. Sci. Pol. Chem.* **55**, 2730–2737 (2017).
23. G. Quintens, J. H. Vrijsen, P. Adriaensens, D. Vanderzande, T. Junkers, Muconic acid esters as bio-based acrylate mimics. *Polym. Chem.* **10**, 5555–5563 (2019).
24. F. J. Vara, J. A. Dougherty, J. S. Plotkin, Furanone/vinyl ether copolymers, U.S. Patent US4954593A, 4 September 1990.
25. V. V. Poskonin, D. N. Yakovlev, V. A. Kovardakov, L. A. Badovskaya, Studies on substituted butane- and butenolides: XIV. Synthesis of high-molecular butanolides on the basis of 4-alkoxy-2-butenolides and vinyl monomers. *Russ. J. Org. Chem.* **35**, 721–726 (1999).
26. P.T. Anastas, J. C. Warner, *Green Chemistry: Theory and Practice* (Oxford Univ. Press, 2000).
27. K. J. Zeitsch, *The Chemistry and Technology of Furfural and Its Many By-Products* (Elsevier, Amsterdam, 2000).
28. J. C. De Jong, B. L. Feringa, Asymmetric Diels-Alder reactions with a chiral maleic anhydride analog, 5-(1-menthyloxy)-2(5H)-furanone. *J. Org. Chem.* **53**, 1125–1127 (1988).
29. A. van Oeveren, B. L. Feringa, Asymmetric synthesis of 5-substituted gamma-lactones and butenolides via nucleophilic additions to oxycarbenium ions derived from 5(R)-(menthyloxy)-4(R)- (phenylsulfanyl)-2(3H)-dihydrofuranone. *J. Org. Chem.* **61**, 2920–2921 (1996).
30. C. Sambiagio, T. Noël, Flow photochemistry: Shine some light on those tubes! *Trends Chem.* **2**, 92–106 (2020).
31. J. Villadsen, J. Nielsen, G. Lidén, Gas–liquid mass transfer, in *Bioreaction Engineering Principles* (Springer, Boston, MA, 2011) pp. 459–496.
32. C. A. Clark, D. S. Lee, S. J. Pickering, M. Poliakoff, M. George, A simple and versatile reactor for photochemistry. *Org. Process Res. Dev.* **20**, 1792–1798 (2016).
33. B. D. A. Hook, W. Dohle, P. R. Hirst, M. Pickworth, M. B. Berry, K. I. Booker-Milburn, A practical flow reactor for continuous organic photochemistry. *J. Org. Chem.* **70**, 7558–7564 (2005).
34. F. Lévesque, P. H. Seeberger, Highly efficient continuous flow reactions using singlet oxygen as a "Green" reagent. *Org. Lett.* **13**, 5008–5011 (2011).
35. A. Yavorskyy, O. Shvydkiv, N. Hoffmann, K. Nolan, M. Oelgemöller, Parallel microflow photochemistry: Process optimization, scale-up, and library synthesis. *Org. Lett.* **14**, 4342–4345 (2012).
36. Y. Su, K. Kuijpers, V. Hessela, T. Noël, A convenient numbering-up strategy for the scale-up of gas–liquid photoredox catalysis in flow. *React. Chem. Eng.* **1**, 73–81 (2016).
37. A. Valdebenito, M. V. Encinas, Effect of solvent on the free radical polymerization of *N,N*-dimethylacrylamide. *Polym. Int.* **59**, 1246–1251 (2010).
38. C. Magee, Y. Sugihara, P. B. Zetterlund, F. Aldabbagh, Chain transfer to solvent in the radical polymerization of structurally diverse acrylamide monomers using straight-chain and branched alcohols as solvents. *Polym. Chem.* **5**, 2259–2265 (2014).
39. R. P.-T. Chung, D. H. Solomon, Recent developments in free-radical polymerization—A mini review. *Prog. Org. Coat.* **21**, 227–254 (1992).
40. S. C. Ligon, B. Husár, H. Wutzel, R. Holman, R. Liska, Strategies to reduce oxygen inhibition in photoinduced polymerization. *Chem. Rev.* **114**, 557–589 (2014).
41. H. G. Viehe, R. Merényi, Z. Janousek, Captodative substituent effects in radical chemistry. *Pure Appl. Chem.* **60**, 1635–1644 (1988).
42. C. Cao, Y. Lin, Correlation between the glass transition temperatures and repeating unit structure for high molecular weight polymers. *J. Chem. Inf. Comput. Sci.* **43**, 643–650 (2003).
43. R. D. Athey, Testing coatings for solvent and chemical resistance. *Metal Finish.* **108**, 359–362 (2010).
44. K. J. van den Berg, L. G. J. van der Ven, H. J. W. van den Haak, Development of waterborne UV-A curable clear coat for car refinishes. *Prog. Org. Coat.* **61**, 110–118 (2008).
45. P. Imhof, J. C. van der Waal, *Catalytic Process Development For Renewable Materials* (Wiley, Weinheim, 2013).
46. R. Sheldon, Green and sustainable manufacture of chemicals from biomass: State of the art. *Green Chem.* **16**, 950–963 (2014).
47. A. B. Pangborn, M. A. Giardello, R. H. Grubbs, R. K. Rosen, F. J. Timmers, Safe and convenient procedure for solvent purification. *Organometallics* **15**, 1518–1520 (1996).
48. G. R. Fulmer, A. J. M. Miller, N. H. Sherden, H. E. Gottlieb, A. Nudelman, B. M. Stoltz, J. E. Bercaw, K. I. Goldberg, NMR chemical shifts of trace impurities: common laboratory solvents, organics, and gases in deuterated solvents relevant to the organometallic chemist. *Organometallics* **29**, 2176–2179 (2010).
49. K. F. O'Driscoll, J. Huang, The rate of copolymerization of styrene and methyl methacrylate—II. The gel effect in copolymerization. *Eur. Polym. J.* **26**, 643–647 (1990).
50. I. M. Barszczewska-Rybarek, A. Korytkowska-Wałach, M. Kurcok, G. Chiladek, J. Kasperski, DMA analysis of the structure of crosslinked poly(methyl methacrylate)s. *Acta Bioeng. Biomech.* **19**, 47–53 (2017).

Acknowledgments: We thank R. Costil and A. S. Lubbe for the fruitful discussions and suggestions, O. K. B. Staal for technical support regarding the photooxidation setups, R. Freeke for help with DSC and DMTA measurements, C. Hermans and L. Brugman for help with GPC measurements, and J. L. Sneep and J. Hekelaar for assistance with HRMS. **Funding:** This work is part of the Advanced Research Center for Chemical Building Blocks, ARC CBBC, which is cofounded and cofinanced by the Netherlands Organization for Scientific Research (NWO, contract 736.000.000) and the Netherlands Ministry of Economic Affairs and Climate. **Author contributions:** B.L.F. conceptualized the research project and coordinated it with the help of K.J.v.d.B. J.G.H.H., T.F., and R.v.G. conducted the research and its validation. J.G.H.H. and B.L.F. prepared the manuscript with input from T.F. and K.J.v.d.B. All authors reviewed the manuscript. **Competing interests:** The authors declare that they have no competing interests. **Data and materials availability:** Additional data can be found in the Supplementary Materials. All data needed to evaluate the conclusions in the paper are present in the paper and/or the Supplementary Materials. Additional data related to this paper may be requested from the authors.

Submitted 24 July 2020
Accepted 30 October 2020
Published 16 December 2020
10.1126/sciadv.abe0026

Citation: J. G. H. Hermens, T. Freese, K. J. van den Berg, R. van Gemert, B. L. Feringa, A coating from nature. *Sci. Adv.* **6**, eabe0026 (2020).